

RoadTrack: Tracking Road Agents in Dense and Heterogeneous Environments

Rohan Chandra¹, Uttaran Bhattacharya¹, Tanmay Randhavane², Aniket Bera², and Dinesh Manocha¹
¹University of Maryland, ²University of North Carolina

Abstract—We present an algorithm to track traffic agents in dense videos. Our approach is designed for heterogeneous traffic scenarios that consist of different agents such as pedestrians, two-wheelers, cars, buses etc. sharing the road. We present a novel Heterogeneous Traffic Motion and Interaction model (HTMI) to predict the motion of agents by modeling collision avoidance and interactions between the agents. We implement HTMI within the tracking-by-detection paradigm and use background subtracted representations of traffic agents to extract binary tensors for accurate tracking. We highlight the performance on a dense traffic videos and observe an accuracy of 75.8%. We observe up to $4\times$ speedup over prior tracking algorithms on standard traffic datasets.

I. INTRODUCTION

Tracking of traffic agents on a highway or an urban road is an important problem in autonomous driving, intelligent transportation, and related areas. These heterogeneous traffic agents may correspond to large or small cars, buses, bicycles, rickshaws, pedestrians, moving carts, etc. Different agents have different shapes, move at varying speeds, and their trajectories are governed by underlying dynamics constraints. Furthermore, the traffic patterns or behaviors can vary considerably between highway traffic, urban traffic or driving in highly congested areas (*e.g.* in some Asian cities).

Given a traffic video, the tracking problem corresponds to computing the consistency in the temporal and spatial identity of all agents in the video frame sequence. Recent developments in autonomous driving and large-scale deployment of high-resolution cameras for surveillance has generated interest in the development of accurate tracking algorithms, especially in dense scenarios with a large number of heterogeneous agents. The complexity of tracking increases as different types of traffic agents come in close proximity and interact with each other. In practice, however, road-agent interactions predominantly involve one or more pedestrians. We therefore mainly consider traffic scenes that necessarily contain pedestrians. Examples of such interactions include passengers boarding or deboarding buses, bicyclists riding alongside cars and so on.

The traffic congestion on highways and urban roads often result in high-density traffic scenarios. The traffic density can be defined based on the number of distinct traffic agents captured in a single frame of the video or the number of agents per unit length of the roadway. It is not uncommon to capture videos with tens or hundreds of traffic agents in a single frame. The high density makes it hard to track all the agents reliably over a sequence of frames.



Fig. 1. We highlight the performance of our tracking algorithm, RoadTrack, in this urban video. This frame consists of 27 traffic-agents, including pedestrians, two-wheel scooters, three-wheel rickshaws, cars, and bicycles. Our algorithm can track agents with 84.8% accuracy at 1-2 fps on a TitanXp GPU. We observe average improvement of 5.2% in MOTA accuracy over prior methods.

To solve the tracking problem in dense and heterogeneous traffic scenarios, we require a motion model that can account for interactions among heterogeneous agents and the high density in which these agents move. We adopt the tracking-by-detection paradigm, which is a two-step process of object detection and state prediction using the motion model. The first step, object detection, is performed to generate vectorized representations, called binary tensors, for each traffic agent that facilitate identity association across frames. The second step is to predict the state (position and velocity) for the next frame using a motion model.

Main Contributions: We present a novel algorithm called RoadTrack to track heterogeneous traffic agents in dense videos. The novel contributions of our work include:

- 1) The “Heterogeneous Traffic Motion and Interaction Model (HTMI)” to model the motion of different traffic agents by accounting for collision avoidance and pairwise interactions. We show it is more suited for dense and heterogeneous traffic scenes as compared to linear or some non-linear motion models.
- 2) A feature extraction method using background subtraction. We use the theoretical result that the resulting binary tensors reduce the number of false negatives and significantly increase the accuracy of our algorithm in dense videos.

Our approach makes no assumption regarding camera mo-

tion, camera view, and even lighting conditions. For example, we show our algorithm works perfectly in heavy moving traffic during night with glare from oncoming traffic (see supplementary video). We have compared the performance with state-of-the-art tracking methods on the KITTI-16 traffic sequence [16] from the MOT benchmark and observe a speedup of $4\times$.

II. RELATED WORK

In this section, we give a brief overview of prior work on object tracking and motion modeling.

A. Pedestrian and Vehicle Tracking

There is extensive work on pedestrian tracking [9], [23]. Bruce et al. [2] and Gong et al. [18] predict pedestrians' motions by estimating their destinations. Liao et al. [27] compute a Voronoi graph from the environment and predicts pedestrian's motion along the edges. Mehran et al. [32] apply the social force model to detect people's abnormal behaviors from videos. Pellegrini et al. [38] use an energy function to build a goal-directed short-term collision-avoidance motion model. Bera et al. [1] use reciprocal velocity obstacles and hybrid motion models to improve the accuracy. All these methods are specifically designed for tracking pedestrian movement.

Vehicle tracking has been studied in computer vision, robotics, and intelligent transportation. Some of the earlier techniques are based on using cameras [56], [12], [11] and laser range finders [55], [48]. The recent developments in autonomous driving have resulted in the development of improved sensors and more sophisticated methods. [39] model dynamic and geometric properties of the tracked vehicles and estimate their positions using a stereo rig mounted on a mobile platform. [13] present an approach to detect and track vehicles in highly dynamic environments. [40], [10] use multiple cameras for tracking all surrounding vehicles. Moras et al. [34] use an occupancy grid framework to manage different sources of uncertainty for more efficient vehicle tracking; Wojke et al. [51] use LiDAR for moving vehicle detection and tracking in unstructured environments. [8] uses a feature-based approach to track the vehicles under varying lighting conditions. Most of these methods focus on vehicle tracking and do not take into account interactions with other traffic agents such as pedestrians or two-wheelers in dense urban environments. For an up-to-date review of tracking-by-detection algorithms, we refer the reader to methods submitted to the MOT benchmark [33].

B. Motion Models

There is substantial work on tracking multiple objects and use of motion models to improve the accuracy [22], [4], [46]. [22] presents an extension to MHT [41] so that it can be used with tracking-by-detection paradigm. [46] uses the constant velocity motion model to join fragmented pedestrian tracks caused by occlusion. However, linear motion models do not work well in dense scenes.



Fig. 2. We show examples of common interactions that take place in dense traffic between heterogeneous agents. In this image, we observe two pedestrian-rickshaw interactions and one pedestrian-pedestrian interaction. All interacting agent pairs are denoted (p_i, p_k) and are marked inside green circles.

RVO [49] is a non-linear motion model that has been used for pedestrian tracking in dense crowd videos. Recently, an extension to RVO has been proposed to explicitly model the trajectories of heterogeneous traffic agents with kinematic constraints [30]. However, this approach relies on hand-crafted functions that may not generalize well to all forms of dense and heterogeneous traffic. Further, RVO does not take into account agents interacting with one another. Our proposed motion model, HTMI, models pairwise interactions and is integrated with deep learning-based object detection that eliminates the need for hand-crafted functions. Other motion models used for tracking include social forces [20], LTA [37], and ATTR [53]. However, these are mainly designed for tracking pedestrians.

C. Traffic Modeling and Navigation

Prior works in transportation engineering and robotics have focused on modeling the movement of vehicles and other road agents [35]. Traffic flow can be modeled using macroscopic [25], [17] or microscopic [21], [45], [31], [36] techniques. Luo et al. [29] propose a cellular automata model to simulate the car and bicycle heterogeneous traffic on an urban road. Chow et al. [6] model dynamic traffic based on the variational formulation of kinematic waves. Recent work in autonomous driving includes modeling human interactions or actions [43]. Our approach to model heterogeneous interactions is designed for dense traffic scenarios and is complimentary to these approaches.

III. HTMI: HETEROGENEOUS TRAFFIC MOTION AND INTERACTIONS

One of the major challenges with tracking heterogeneous agents in dense traffic is that agents such as cars, buses, bicycles, agents, etc. have different sizes, geometric shape, maneuverability, behavior, and dynamics. These often lead to complex inter-agent interactions that have not usually been taken into account by prior multi-object trackers. Figure 2 shows common examples of such interactions, such as a

pedestrian approaching a rickshaw to board it, or attempting to move towards another pedestrian while avoiding other agents. Furthermore, traffic-agents in high-density scenarios are in close-proximity to one another or are almost colliding. So we need an efficient approach to model the collisions and interactions. We present a novel HTMI model that takes into account both

- Reciprocal collision avoidance [49] with car-like kinematic constraints for trajectory prediction and collision avoidance.
- Heterogeneous agent interaction that predicts when two or more agents will interact with each other in the near future.

All the notations used in the paper are highlighted in Table I.

A. Collision Avoidance

Reciprocal Velocity Obstacles (RVO) [49] extends Velocity Obstacles motion model by modeling collision avoidance behavior for multiple engaging agents. RVO can be applied to pedestrians in a crowd and we modify it to work with bounding boxes as our algorithm conforms to the tracking-by-detection paradigm.

We represent each agent as, $\Psi_t = [u, v, \dot{u}, \dot{v}, v_{\text{pref}}]$, where u, v, \dot{u}, \dot{v} , and v_{pref} represent the top left corner of the bounding box, their velocities, and the preferred velocity of the agent in the absence of obstacles respectively. v_{pref} is computed internally by RVO.

The computation of the new state, Ψ_{t+1} , is expressed as an optimization problem. For each agent, RVO computes a feasible region where it can move without collision. This region is defined according to the RVO collision avoidance constraints (or ORCA constraints [49]). If the ORCA constraints forbid an agent's preferred velocity, that agent chooses the velocity closest to its preferred velocity that lies in the feasible region, as given by the following optimization:

$$v_{\text{new}} = \arg \min_{v \notin \text{ORCA}} \|v - v_{\text{pref}}\| \quad (1)$$

The velocity, v_{new} , is then used to calculate the new position of a traffic agent.

The difference in shapes, sizes, and aspect ratios of agents motivate the need to use appearance-based binary tensors. In order to combine object detection with RVO, we modify the state vector, Ψ_t , to include bounding box information by setting the position to the centers of the bounding boxes. Thus $u \leftarrow \frac{u+w}{2}, v \leftarrow \frac{v+h}{2}$.

B. Heterogeneous Agent Interactions

In a traffic scenario, interactions can occur between different types of agents: vehicle-vehicle, pedestrian-pedestrian, vehicle-pedestrian, bicycle-pedestrian, etc. In this section, we present a formulation to model such interactions.

The authors in [19] proposed the idea of spatial regions that dictate human behavior, specifically, the public and the social regions. In Figure 3, the yellow area is the social region and the orange area is the public region. Based on

this work, [44] proposed a model of approach behavior with which a robot can interact with humans. At the public distance the robot is allowed to approach the human to interact with them, and at the social distance, interaction occurs. We adopt these ideas into HTMI and posit that in order to predict the new velocity, v_{new} , an agent follows three steps:

1) *Intent of Interaction*: An agent p_i intends to interact with another agent p_k when p_i is within the social distance of p_k for some minimum time τ . When two traffic agents intend to interact, they move towards each other and come in close proximity. This can roughly be viewed as ‘‘complementary’’ to motion modeling for collision avoidance.

2) *Ability to Interact*: Even when two agents want to interact, their movements could be restricted in dense traffic. We determine the ability to interact (Figure 3(right)) as follows.

Each agent has a personal space, which we define as a circular region, ζ of radius ρ , centered around p_k . Given a traffic agent p_i , the slope of its v_{pref} is $\tan \theta$. θ is the angle with the horizontal defined in the world coordinate system. In dense traffic, each agent, p_i has a limited space in which they can steer, or turn. This space is the feasible region determined by the ORCA constraints described in the previous section. We define a 2D cone, γ , of angle ϕ as the ORCA region in which the agent can steer. ϕ is thus the steering angle of the agent. We denote the extreme rays of the cone as r_1 and r_2 . $\perp_{g_1}^{g_2}$ denotes the smallest perpendicular distance between two geometric structures, g_1 and g_2 . These parameters are fixed for different agent types and are not learned from data.

If p_i has intended to interact with p_k , the projected cone of p_i , defined by extending r_1 and r_2 , is directed towards p_k . Then, in order for interaction to take place, it is sufficient to check for either one of two conditions to be true:

- 1) Intersection of ζ with either r_1 or r_2 (if either ray intersects, then the entire cone intersects ζ).
- 2) $\zeta \subset \gamma$ (if ζ lies in the interior of the cone, see Figure 3).

For these conditions to hold, we require that the cone does not intersect or contain any $p_j \in \mathcal{A}, j \neq i$. We now make these equations more explicit.

We parameterize r_1, r_2 by their slopes $\tan \delta$, where $\delta = \theta_i + \phi_i$ if $\perp_{\zeta}^{r_1} \geq \perp_{\zeta}^{r_2}$, else $\delta = \theta_i - \phi_i$. The resulting equation of r_1 (or r_2) is,

$$(Y - v_i) = \tan \delta (X - u_i) \quad (2)$$

and the equation of ζ is,

$$(X - u_k)^2 + (Y - v_k)^2 = \rho^2 \quad (3)$$

Solving both equations simultaneously, we obtain an equation, Ω_1 . Intersection occurs if the discriminant of $\Omega_1 \geq 0$. This provides us with the first condition necessary for the occurrence of an interaction between p_i and p_k .

Next, we observe that if ζ lies in the interior of γ , then p_k lies on the opposite sides of r_1 and r_2 which is modeled by the following equation:

$$\Omega_2 \equiv r_1(p_k).r_2(p_k) \leq 0 \quad (4)$$

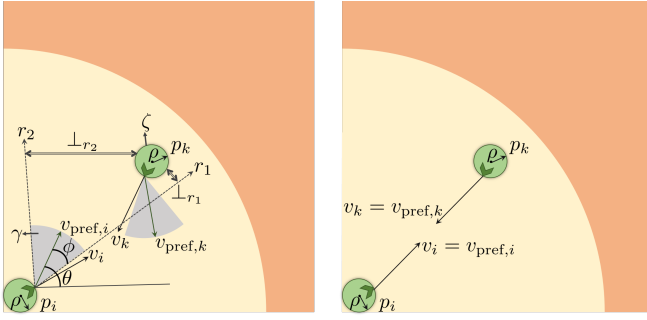


Fig. 3. Inner yellow circle denotes the social distance and the outer orange area denotes the public region. At time $t \geq \tau$ and using III-B.1, p_i intends to interact with p_k . Then using III-B.2 (left), p_i determines its ability to interact with p_k . We observe that γ (grey cone) of p_i contains ζ of p_k (green circle around p_k). Thus p_i can interact with p_k . Using III-B.3 (right), p_i and p_k align their preferred velocities toward each other.

Solving Equation 4 further provides us with the second condition for the occurrence of an interaction between p_i and p_k , where $\Omega_1, \Omega_2 : \mathbb{R}^2 \times \mathbb{R}^2 \times \mathbb{R} \times \mathbb{R} \mapsto \mathbb{R}$.

3) *Interaction*: If either Ω_1 or Ω_2 is true, then agents p_i, p_k will move towards each other to interact at time $t \geq \tau$. When this happens, we assume that p_i and p_k align their current velocities towards each other. Thus,

$$v_{\text{new}} = v_{\text{pref}} \quad (5)$$

The time taken for the two agents to be meet or converge with each other is given by:

$$t = \frac{\|p_i - p_k\|_2}{\|v_i - v_k\|_2} \quad (6)$$

If two agents are overlapping (based on the values of Ω_1 and Ω_2), we model them as a new agent with radius 2ϵ .

Our approach can be extended to model multiple interactions. We form a set $\mathcal{I} \subseteq \mathcal{A}$, where \mathcal{I} is the set of all agents a_ω , that are intending to interact with p_k . In order to determine the first agent that may interact with p_k , we can compute the time taken by that agent as: $t_{\min} = \arg \min_t \|v_\omega t - p_k\| = \rho, p_\omega \in \mathcal{I}$. Agents that are not interacting avoid each other and continue moving towards their destination.

To summarize, HTMI predicts the new velocity of an agent by accounting for collision avoidance and interactions. For collision avoidance, HTMI modifies RVO to incorporate bounding box information. HTMI further formulates when and how two agents can interact in a densely crowded traffic scene. We model the time taken by that agent to reach the other agent, and we also take into account multiple interactions in the same scene. HTMI is integrated within the tracking-by-detection paradigm and we use the new positions and velocities in conjunction with object detection and segmentation to perform accurate tracking.

C. Analysis

We analyze the performance of HTMI in traffic scenarios with increasing density and heterogeneity. In this section, we

analytically show the advantage of HTMI over other motion models such as Social Forces [20], RVO [49], and constant velocity [50].

We denote the multiple object tracking accuracy, $MOTA$ of a system using a particular motion model as $MOTA^{\text{model}}$ and define it as,

$$MOTA^{\text{model}} = \sum_c MOTA_c + \sum_i MOTA_i \quad (7)$$

where c and i denote an agent whose motion is being modeled using collision avoidance and interaction, and $MOTA_c$ and $MOTA_i$ denote their individual accuracies, respectively. Let n represent the number of total agents in a video. We define $H(n)$ as the ‘‘Heterogeneity Index’’ and it is defined as,

$$\text{Definition III.1. Heterogeneity Index: } H(n) = \max_h n_{\text{category}} \geq h \text{ such that } |\text{category}| \geq 2.$$

where category represents the type of an agent such as pedestrians, cars, and so on. For example, a scenario containing 3 cars, 4 pedestrians, and 2 buses would have a heterogeneity index of 2. It also follows that $n = \sum_{\text{category}} n_{\text{category}}$.

It is reasonable to assume that a higher $H(n)$ would increase the number of agents whose motion is modeled through collision avoidance and heterogeneous interaction formulations. Linear models do not account for either formulation. Standard RVO only accounts for collision avoidance. HTMI models both. Therefore, we posit that,

$$\begin{aligned} MOTA_c^{\text{linear}} &\leq MOTA_c^{\text{RVO}} \approx MOTA_c^{\text{HTMI}} \\ MOTA_i^{\text{linear}} &\leq MOTA_i^{\text{RVO}} \leq MOTA_i^{\text{HTMI}} \\ \Rightarrow MOTA^{\text{linear}} &\leq MOTA^{\text{RVO}} \leq MOTA^{\text{HTMI}} \end{aligned} \quad (8)$$

Observe that increasing $H(n)$ implies that n increases as well, although the converse may not be true. This observation further supports our claim that HTMI achieves higher accuracy in more heterogeneous and denser traffic scenarios. We validate the analysis presented here in Section V-C.

IV. ROADTRACK AND BGS-REPRESENTATION

In this section, we present our novel tracking-by-detection algorithm that combines Mask R-CNN with a novel heterogeneous interaction model.

RoadTrack uses Mask R-CNN for agent detection and is integrated with HTMI for motion modeling. We use a tensor extraction method based on background subtraction. The binary tensors generated are compared using association algorithms [24] to compute the ID of each agent in the next frame. We illustrate our approach in Figure 4. At current time t , given the ID labels of all agents in the frame, we want to assign labels for agents at time $t+1$. We start by using Mask R-CNN to implicitly perform pixel-wise agent segmentation to generate ‘‘BGS-Representations’’. These are boxes similar to regular bounding boxes but with background subtraction. Next, we predict the spatial coordinates for each agent for

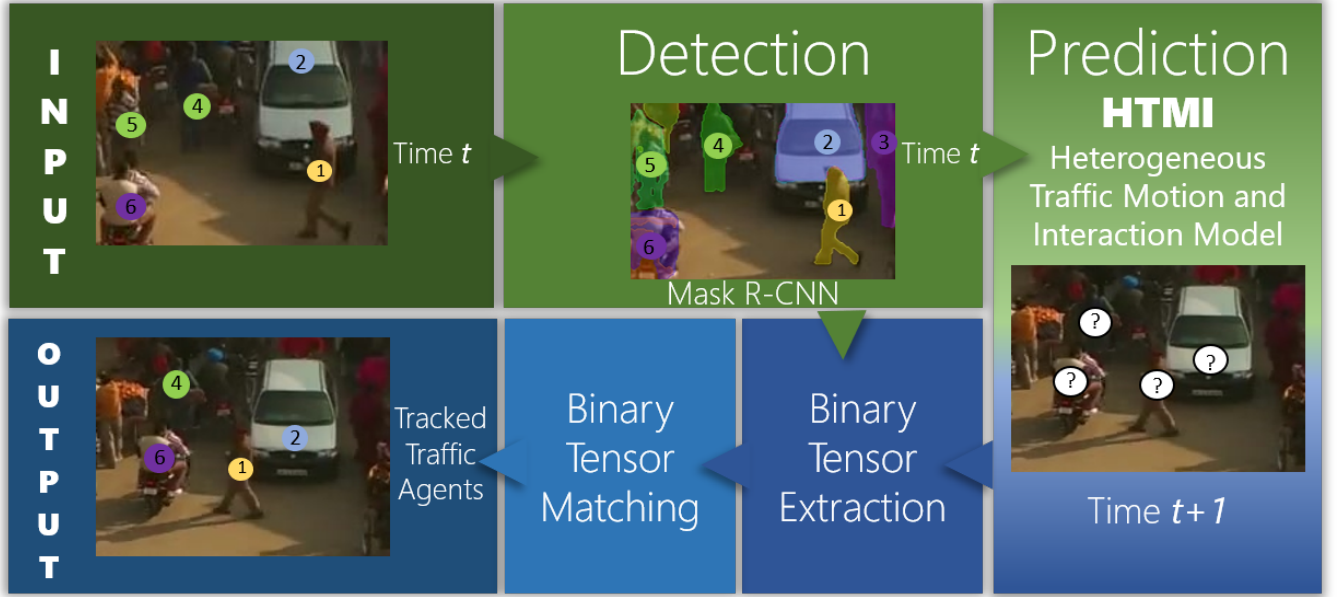


Fig. 4. Overview of RoadTrack: We use Mask R-CNN on an input frame at time t to generate background subtracted (BGS) representations of agents. We use our novel motion and interaction model, HTMI, to predict the agent’s state at frame $t + 1$. We generate binary tensors that are invariant to shape, size and scale of heterogeneous agents. These features are matched using association algorithms and a tracking ID is assigned to each predicted agent based on feature matching.

Symbol	Description
p_i	i^{th} agent
h_j	j^{th} detected agent (ie, it has a bounding box)
\mathcal{A}	set of all agents in the current frame
\mathcal{H}	set of all detected agents in the current frame
\mathcal{H}_i	subset of all detected agents in the current frame that are within a circular region around agent p_i
\mathbb{B}_{p_j}	bounding box for detected agent h_j
$p_i \equiv (u_i, v_i)$	position of p_i , similarly defined for p_k
$v_i \equiv (\dot{u}_i, \dot{v}_i)$	velocity of p_i , similarly defined for a_k
f_{p_i}	feature vectors of the predicted agent, p_i .
f_{h_j}	feature vectors of the segmented representation, h_j
$l(p, q)$	cosine metric defined by $1 - p^T q$
ψ_t	state of an agent p_i at time t , includes position, velocity, and preferred velocity

TABLE I
NOTATIONS USED IN THE PAPER.



Fig. 5. An extremely dense traffic scene with 36 agents. We use Mask R-CNN to perform background subtractions on pedestrians, rickshaws, and cars for accurate tracking.

the next time-step using HTMI. This results in another set of BGS-Representations for each agent at time $t + 1$.

We use these sets of BGS-Representations to compute binary tensors using a Convolutional Neural Network [50]. The binary tensors are matched in two ways: the Cosine metric and the IoU overlap [26]. The Cosine metric is computed using the following optimization problem:

$$h_{j,p_i}^* = \arg \min_{h_j} (l(f_{a_i}, f_{h_j}) | p_i \in \mathcal{P}, h_j \in \mathcal{H}_i). \quad (9)$$

The IoU overlap metric is used in conjunction with the cosine metric. This metric builds a cost matrix Σ to measure the amount of overlap of each predicted bounding box with all nearby detection bounding box candidates. $\Sigma(i, j)$ stores the

IoU overlap of the bounding box of Ψ_{t+1,p_i} with that of h_j and is calculated as:

$$\Sigma(i, j) = \frac{\mathbb{B}_{\Psi_{t+1,p_i}} \cap \mathbb{B}_{h_j}}{\mathbb{B}_{\Psi_{t+1,p_i}} \cup \mathbb{B}_{h_j}}, h_j \in \mathcal{H}_i. \quad (10)$$

Matching a detection to a predicted measurement with maximum overlap thus becomes a max-weight matching problem and we solve it efficiently using the Hungarian algorithm [24]. The ID of the agent at time t is assigned to the agent at time $t + 1$ whose appearance is most closely associated to the agent at time t .

A. BGS-Representations Using Mask R-CNN

One of the challenges in detecting agents in dense traffic videos is that the bounding boxes often overlap. This in-

creases noise in bounding boxes of individual agents. To address this, we use Mask R-CNN to perform pixel-wise agent segmentation, thereby subtracting the noisy background from the original bounding box (Figure 5). In practice, Mask R-CNN essentially segments out the agent from its bounding box, and thereby reduce the noise that occurs when the agents are in close proximity.

Mask R-CNN generates a bounding box and its corresponding mask for each detected agent in each frame. We create a white canvas and superimpose a pixel-wise segmented agent onto the canvas using the mask. We perform detection in \mathbb{F}_t and the output consists of bounding boxes, masks, scores, and class IDs of agents at current time t .

$\mathcal{B} = \{\mathbb{B}_{h_j} \mid \mathbb{B} = [\langle x, y \rangle_{\text{top left}}, w, h, s, r], h_j \in \mathcal{H}\}$ denotes the set of bounding boxes for each h_j at current time t , where $\langle x, y \rangle_{\text{top left}}, w, h, s$, and r denote the top left corner, width, height, scale, and aspect ratio of \mathbb{B}_j , respectively.

$\mathcal{M} = \{\mathbb{M}_{h_j} \mid h_j \in \mathcal{H}\}$ denotes the set of masks for each h_j in \mathbb{F}_t , where each \mathbb{M}_{h_j} is a $[w \times h]$ tensor of boolean variables.

Let $\mathcal{W} = \{\mathbb{W}_{h_j}(\cdot) \mid h_j \in \mathcal{H}\}$ be the set of white canvases where each canvas, $\mathbb{W}_{h_j} = [\mathbb{1}]_{w \times h}$, w and h are the width and height of each \mathbb{B}_{h_j} at current time t . Then,

$$\mathcal{U} = \{\mathbb{W}_{h_j}(\mathbb{M}_{h_j}) \mid \mathbb{W} \in \mathcal{W}, \mathbb{M} \in \mathcal{M}, h_j \in \mathcal{H}\}$$

is the set of BGS-representations for each h_j at current time t . These BGS-representations are used to compute binary tensors. We then use the following theorem.

Theorem IV.1. *With high probability, binary tensors extracted from background subtracted (BGS) representations decrease the number of road agent tracks lost, thereby reducing the number of false negatives.¹*

V. RESULTS

In this section, we highlight the performance of RoadTrack through extensive experiments on different datasets.

A. On Dense Datasets

We use the TRAF dataset [3] that consists of a set of 50 video sequences that contain dense traffic with highly heterogeneous agents with varying viewpoints, camera motions, and at different times of the day. These videos are of highway and urban traffic in China, and India. Most importantly, ground truth annotations consisting of 2-D bounding box coordinates and agent types are provided with the dataset. The key aspects of this dataset are the density and the degree of heterogeneity. Compared to standard traffic datasets such as KITTI [16] and PETS[15], this dataset is denser with a higher degree of heterogeneity.

We provide baseline results on the TRAF dataset using our tracking algorithm, RoadTrack, and demonstrate a high average MOTA of 75.8% (Table II). We compute the accuracy (MOTA) according to the CLEAR metrics [47] as $MOTA =$

¹For the interested reader, the proof of this theorem is located at https://rohanchandra30.github.io/attachments/ROS19_Chandra.pdf

$\frac{1-(FN+FP+IDS)}{GT}$, where FN, FP, IDS, and GT correspond to the number of false negatives, false positives, ID switches, and ground truth agents, respectively. Additionally, we report the number of mostly tracked (MT) and mostly lost (ML) agents as well as the precision of the detector (MOTP), as per their provided definitions in [47]. We do not count stationary agents such as parked vehicles in our formulation. Detected objects such as traffic signals are considered false positives. We take into account all possible road agents. RoadTrack can be optimized further by sub-sampling and using parallelization to increase the frame rate.

We compare RoadTrack with other methods on dense datasets in Table II. MOTDT [28] and MDP [52] are the only state-of-the-art methods with available open-source code. Compared to these methods, we reduce false negatives by 18.1% relatively and improve upon MOTA by 5.2% on absolute. This is roughly equivalent to a rank difference of 46 on the MOT benchmark.

Note that we observe an abnormally high number of identity switches compared to other methods; however, this is because prior methods mostly fail to maintain an agent’s track for more than 20% of their total visible time (near 100% ML). Not being able to track agents for most of the time consequently results in lower IDS for prior methods. However, the low IDS score for prior methods also contributes to their reasonably high MOTA score, despite near-failure to track agents in dense traffic.

B. On Standard Benchmark

The current state-of-the-art standard tracking benchmark is the MOT benchmark, which contains a mix of pedestrians and traffic sequences. We select the traffic sequence KITTI-16 [16] since it is the most relevant sequence for RoadTrack, and compare with top-performing online methods that have an average rank higher than ours. However, it should be noted that the KITTI sequence is sparse with a low degree of heterogeneity.

As RoadTrack is primarily designed for dense traffic, we neither claim nor observe it to outperform prior methods on the sparse KITTI-16 sequence. We specifically observe a low MOTA score which we attribute to a high number of false positives given by the detector. These false positives are largely due to valid traffic agents not annotated in the ground truth sequence. However, we achieve the lowest number of false negatives, which is a direct consequence of our BGS-Representation.

C. Ablation Experiments

We highlight the advantages of HTMI and using binary tensors generated from BGS-Representations through ablation experiments in Table IV. We compare with the following variations of RoadTrack.

- Constant Velocity (Const. Vel). We replace HTMI with a constant velocity motion model [50].
- Social Forces (SF). We replace HTMI with the Social Forces motion model [20].

Dataset	Tracker	MT(%) \uparrow	ML(%) \downarrow	IDS \downarrow	FN \downarrow	MOTP(%) \uparrow	MOTA(%) \uparrow
TRAF1	MOTDT	0	98.2	15 (<0.1%)	18,764 (33.0%)	63.3	67.0
	MDP	0	98.2	21 (<0.1%)	18,667 (32.8%)	60.1	67.1
	RoadTrack	0	95.6	163 (0.3%)	17,953 (31.6%)	58.8	68.1
TRAF2	MOTDT	0	98.8	17 (<0.1%)	18,201 (32.7%)	60.3	67.3
	MDP	0	100.0	7 (<0.1%)	18,105 (32.5%)	59.6	67.5
	RoadTrack	0	92.3	55 (0.1%)	17,202 (30.9%)	60.8	69.0
TRAF3	MOTDT	3.3	67.1	64 (<0.1%)	34,883 (27.0%)	69.6	72.9
	MDP	0	100.0	0 (0.0%)	43,057 (33.3%)	69.2	66.7
	RoadTrack	32.2	40.0	62 (<0.1%)	19,521 (15.1%)	70.1	84.8
TRAF4	MOTDT	1.2	76.3	123 (0.1%)	54,849 (29.0%)	65.3	70.9
	MDP	1.2	87.2	16 (<0.1%)	59,097 (31.3%)	66.2	68.7
	RoadTrack	6.0	54.6	266 (0.1%)	47,444 (25.1%)	65.1	74.7
TRAF5	MOTDT	0.7	75.9	221 (0.2%)	33,774 (28.9%)	63.2	70.9
	MDP	0	98.4	6 (<0.1%)	38,091 (32.6%)	64.9	67.3
	RoadTrack	1.5	55.7	299 (0.3%)	24,860 (21.3%)	63.1	78.4
TRAF6	MOTDT	0	87.5	161 (0.1%)	58,212 (29.4%)	63.3	70.5
	MDP	0	99.3	0 (0.0%)	65,687 (33.2%)	68.6	66.8
	RoadTrack	0.7	67.8	283 (0.1%)	52,017 (26.3%)	62.8	73.6
Summary	MOTDT	0.9	83.6	601 (0.1%)	218,683 (29.3%)	65.5	70.6
	MDP	0.2	97.0	50 (<0.1%)	242,704 (32.6%)	65.3	67.4
	RoadTrack	7.0	66.9	1128 (0.2%)	178,997 (24.0%)	65.7	75.8

TABLE II

EVALUATION ON OUR DATASET WITH MOTDT [28] AND MDP [52]. MOTDT IS CURRENTLY THE BEST *online* TRACKER ON THE MOT BENCHMARK WITH OPEN-SOURCED CODE. BOLD IS BEST. ARROWS (\uparrow , \downarrow) INDICATE THE DIRECTION OF BETTER PERFORMANCE. **OBSERVATION:** ROADTRACK IMPROVES THE ACCURACY (MOTA) OVER THE STATE-OF-THE-ART BY 5.2% AND PRECISION (MOTP) BY 0.2%. WE REDUCE THE NUMBER OF FALSE NEGATIVES (FN) BY 18% COMPARED TO THE NEXT BEST METHOD, WHICH IS A DIRECT CONSEQUENCE OF USING OUR BGS-REPRESENTATION.

	Tracker	Hz \uparrow	MT(%) \uparrow	ML(%) \downarrow	IDS \downarrow	FN \downarrow	MOTA(%) \uparrow
KITTI-16	AP_HWDPL_p [5]	6.7	17.6	11.8	18	831	40.7
	RAR_15_pub [14]	5.4	0.0	17.6	18	809	41.2
	AMIR15 [42]	1.9	11.8	11.8	18	714	50.4
	HybridDAT [54]	4.6	5.9	17.6	10	706	46.3
	AM [7]	0.5	5.9	17.6	19	805	40.6
	RoadTrack	28.9	29.4	11.7	15	668	12.2

TABLE III

EVALUATION ON THE KITTI-16 SEQUENCE FROM THE MOT15 BENCHMARK WITH *online methods* THAT HAVE AN AVERAGE RANK HIGHER THAN OURS. ROADTRACK IS UP TO 4 \times FASTER THAN STATE-OF-THE-ART. BOLD IS BEST, BLUE IS SECOND BEST. ARROWS (\uparrow , \downarrow) INDICATE THE DIRECTION OF BETTER PERFORMANCE.

Tracker	MT(%) \uparrow	ML(%) \downarrow	IDS \downarrow	FN \downarrow	MOTP(%) \uparrow	MOTA(%) \uparrow
BBox	14.0	44.7	313	34,716	76.4	17.6
RoadTrack	19.0	32.7	429	27,499	75.6	20.0
Const. Vel	0.0	100	11	247,738(33.3%)	66.3	66.7
SF	0.1	98.6	147	246,528 (33.1%)	63.8	66.3
RVO	0.0	100	38	247,675 (33.2%)	63.8	66.9
RoadTrack	7.0	66.9	1128	178,997 (24.0%)	65.7	75.8

TABLE IV

ABLATION EXPERIMENTS WHERE WE DEMONSTRATE THE ADVANTAGE OF HTMI AND BGS-REPRESENTATIONS. WE REPLACE THE HTMI WITH A CONSTANT VELOCITY (CONST. VEL) [50], SOCIAL FORCES (SF) [20], AND RVO MOTION MODEL (RVO)[49] AND WE REPLACE BS-REPRESENTATIONS WITH REGULAR BOUNDING BOXES (BBOX). THE REST OF THE METHOD IS IDENTICAL TO THE ORIGINAL METHOD. BOLD IS BEST. ARROWS (\uparrow , \downarrow) INDICATE THE DIRECTION OF BETTER PERFORMANCE.

- Reciprocal Velocity Obstacles (RVO) [49]. We use RVO instead of HTMI.
- Bounding Boxes (Bbox). We replace BGS-Representations with regular bounding boxes without background subtraction.

We compare HTMI with other motion models (Constant velocity, Social Forces, and RVO) on the dense TRAF dataset. We observe that HTMI outperforms the motion

models by at least 8.9% on absolute on MOTA. We experimentally verify the analysis of Section III-C by observing that $MOTA_{Const.Vel} < MOTA_{RVO} < MOTA_{HTMI}$. We decrease false negatives by 27.4% relatively, showcasing the advantage of our BGS-Representation. Once again, we point to our high IDS in Table IV, compared to the IDS of other motion models. As mentioned in V, this is due to the near-failure of other motion models (near 100% ML) to track

road agents in dense traffic. Furthermore, replacing our BGS-representations with regular bounding boxes also increases false negatives by 26.2% relatively.

REFERENCES

- [1] Aniket Bera and Dinesh Manocha. REACH: Realtime crowd tracking using a hybrid motion model. *ICRA*, 2015.
- [2] A. Bruce and G. Gordon. Better motion prediction for people-tracking. In *Proc. of the International Conference on Robotics and Automation (ICRA), New Orleans, USA*, 2004.
- [3] Rohan Chandra, Uttaran Bhattacharya, Aniket Bera, and Dinesh Manocha. Taphic: Trajectory prediction in dense and heterogeneous traffic using weighted interactions. *CoRR*, abs/1812.04767, 2018.
- [4] Jiahui Chen, Hao Sheng, Yang Zhang, and Zhang Xiong. Enhancing detection model for multiple hypothesis tracking. In *Conf. on Computer Vision and Pattern Recognition Workshops*, pages 2143–2152, 2017.
- [5] Long Chen, Haizhou Ai, Chong Shang, Zijie Zhuang, and Bo Bai. Online multi-object tracking with convolutional neural networks. In *Image Processing (ICIP), 2017 IEEE International Conference on*, pages 645–649. IEEE, 2017.
- [6] Andy HF Chow, Shuai Li, WY Szeto, and David ZW Wang. Modelling urban traffic dynamics based upon the variational formulation of kinematic waves. *Transportmetrica B: Transport Dynamics*, 3(3):169–191, 2015.
- [7] Qi Chu, Wanli Ouyang, Hongsheng Li, Xiaogang Wang, Bin Liu, and Nenghai Yu. Online multi-object tracking using cnn-based single object tracker with spatial-temporal attention mechanism. In *2017 IEEE International Conference on Computer Vision (ICCV)(Oct 2017)*, pages 4846–4855, 2017.
- [8] Benjamin Coifman, David Beymer, Philip McLauchlan, and Jitendra Malik. A real-time computer vision system for vehicle tracking and traffic surveillance. *Transportation Research Part C: Emerging Technologies*, 6(4):271–288, 1998.
- [9] J. Cui, H. Zha, H. Zhao, and R. Shibasaki. Tracking multiple people using laser and vision. In *Proc. of the IEEE/RSI International Conference on Intelligent Robots and Systems (IROS)*, pages 2116–2121. IEEE, 2005.
- [10] Michael Darms, Paul Rybski, and Chris Urmson. Classification and tracking of dynamic objects with multiple sensors for autonomous driving in urban environments. In *Intelligent Vehicles Symposium, 2008 IEEE*, pages 1197–1202. IEEE, 2008.
- [11] Frank Dellaert and Chuck Thorpe. Robust car tracking using kalman filtering and bayesian templates. In *Conference on intelligent transportation systems*, volume 1, 1997.
- [12] Ernst D Dickmanns. Vehicles capable of dynamic vision: a new breed of technical beings? *Artificial Intelligence*, 103(1-2):49–76, 1998.
- [13] Andreas Ess, Konrad Schindler, Bastian Leibe, and Luc Van Gool. Object detection and tracking for autonomous navigation in dynamic environments. *The International Journal of Robotics Research*, 29(14):1707–1725, 2010.
- [14] Kuan Fang, Yu Xiang, Xiaocheng Li, and Silvio Savarese. Recurrent autoregressive networks for online multi-object tracking. pages 466–475, 2018.
- [15] J Ferryman and Ali Shahrokni. Pets2009: Dataset and challenge. In *2009 Twelfth IEEE International Workshop on Performance Evaluation of Tracking and Surveillance*, pages 1–6. IEEE, 2009.
- [16] Andreas Geiger, Philip Lenz, and Raquel Urtasun. Are we ready for autonomous driving? the kitti vision benchmark suite. In *Conference on Computer Vision and Pattern Recognition (CVPR)*, 2012.
- [17] Nikolas Geroliminis, Carlos F Daganzo, et al. Macroscopic modeling of traffic in cities. In *86th Annual Meeting of the Transportation Research Board, Washington, DC*, 2007.
- [18] Haifeng Gong, Jack Sim, Maxim Likhachev, and Jianbo Shi. Multi-hypothesis motion planning for visual object tracking. pages 619–626, 2011.
- [19] Edward Twitchell Hall. *The hidden dimension*, volume 609. Garden City, NY: Doubleday, 1966.
- [20] Dirk Helbing and Peter Molnar. Social force model for pedestrian dynamics. *Physical review E*, 51(5):4282, 1995.
- [21] Boris S Kerner, Sergey L Klenov, and Dietrich E Wolf. Cellular automata approach to three-phase traffic theory. *Journal of Physics A: Mathematical and General*, 35(47):9971, 2002.
- [22] Chanho Kim, Fuxin Li, Arridhana Ciptadi, and James M Rehg. Multiple hypothesis tracking revisited. In *Proceedings of the IEEE International Conference on Computer Vision*, pages 4696–4704, 2015.
- [23] L. Kratz and K. Nishino. Tracking pedestrians using local spatio-temporal motion patterns in extremely crowded scenes. *Pattern Analysis and Machine Intelligence, IEEE Transactions on*, (99):11, 2011.
- [24] Harold W Kuhn. The hungarian method for the assignment problem. In *50 Years of Integer Programming 1958-2008*, pages 29–47. Springer, 2010.
- [25] Jean-Patrick Lebacque. First-order macroscopic traffic flow models: Intersection modeling, network modeling. In *Transportation and Traffic Theory. Flow, Dynamics and Human Interaction. 16th International Symposium on Transportation and Traffic Theory University of Maryland, College Park*, 2005.
- [26] Michael Levandowsky and David Winter. Distance between sets. *Nature*, 234(5323):34, 1971.
- [27] L. Liao, D. Fox, J. Hightower, H. Kautz, and D. Schulz. Voronoi tracking: Location estimation using sparse and noisy sensor data. In *IROS*, 2003.
- [28] Chen Long, Ai Haizhou, Zhuang Zijie, and Shang Chong. Real-time multiple people tracking with deeply learned candidate selection and person re-identification. In *ICME*, 2018.
- [29] Yongji Luo, Bin Jia, Jun Liu, William HK Lam, Xingang Li, and Ziyou Gao. Modeling the interactions between car and bicycle in heterogeneous traffic. *Journal of advanced transportation*, 49(1):29–47, 2015.
- [30] Yuexin Ma, Dinesh Manocha, and Wenping Wang. Autorvo: Local navigation with dynamic constraints in dense heterogeneous traffic. *arXiv preprint arXiv:1804.02915*, 2018.
- [31] Sven Maerivoet and Bart De Moor. Cellular automata models of road traffic. *Physics Reports*, 419(1):1–64, 2005.
- [32] R. Mehran, A. Oyama, and M. Shah. Abnormal crowd behavior detection using social force model. In *Proc. of the IEEE Conference on Computer Vision and Pattern Recognition, CVPR*, pages 935–942, 2009.
- [33] Anton Milan, Laura Leal-Taixé, Ian Reid, Stefan Roth, and Konrad Schindler. Mot16: A benchmark for multi-object tracking. *arXiv preprint arXiv:1603.00831*, 2016.
- [34] Julien Moras, Véronique Cherfaoui, and Philippe Bonnifait. Credibilist occupancy grids for vehicle perception in dynamic environments. In *Robotics and Automation (ICRA), 2011 IEEE International Conference on*, pages 84–89. IEEE, 2011.
- [35] Brian Paden, Michal Čáp, Sze Zheng Yong, Dmitry Yershov, and Emilio Frazzoli. A survey of motion planning and control techniques for self-driving urban vehicles. *IEEE Transactions on intelligent vehicles*, 1(1):33–55, 2016.
- [36] Gaurav Pandey, K Ramachandra Rao, and Dinesh Mohan. A review of cellular automata model for heterogeneous traffic conditions. In *Traffic and Granular Flow'13*, pages 471–478. Springer, 2015.
- [37] S. Pellegrini, A. Ess, K. Schindler, and L. van Gool. You'll never walk alone: Modeling social behavior for multi-target tracking. In *2009 IEEE 12th International Conference on Computer Vision*, pages 261–268, Sept 2009.
- [38] Stefano Pellegrini, Andreas Ess, Konrad Schindler, and Luc Van Gool. You'll never walk alone: Modeling social behavior for multi-target tracking. In *ICCV*, 2009.
- [39] Anna Petrovskaya and Sebastian Thrun. Model based vehicle detection and tracking for autonomous urban driving. *Autonomous Robots*, 26(2-3):123–139, 2009.
- [40] Akshay Ranges and Mohan M Trivedi. No blind spots: Full-surround multi-object tracking for autonomous vehicles using cameras & lidars. *arXiv preprint arXiv:1802.08755*, 2018.
- [41] Donald Reid et al. An algorithm for tracking multiple targets. *IEEE transactions on Automatic Control*, 24(6):843–854, 1979.
- [42] Amir Sadeghian, Alexandre Alahi, and Silvio Savarese. Tracking the untrackable: Learning to track multiple cues with long-term dependencies.
- [43] Dorsa Sadigh, Shankar Sastry, Sanjit A Seshia, and Anca D Dragan. Planning for autonomous cars that leverage effects on human actions. In *Robotics: Science and Systems*, 2016.
- [44] Satoru Satake, Takayuki Kanda, Dylan F Glas, Michita Imai, Hiroshi Ishiguro, and Norihiro Hagita. How to approach humans?: strategies for social robots to initiate interaction. In *Proceedings of the 4th*

- ACM/IEEE international conference on Human robot interaction*, pages 109–116. ACM, 2009.
- [45] Andreas Schadschneider. Traffic flow: a statistical physics point of view. *Physica A: Statistical Mechanics and its Applications*, 313(1-2):153–187, 2002.
- [46] Hao Sheng, Li Hao, Jiahui Chen, Yang Zhang, and Wei Ke. Robust local effective matching model for multi-target tracking. In *Pacific Rim Conference on Multimedia*, pages 233–243. Springer, 2017.
- [47] Arnold WM Smeulders, Dung M Chu, Rita Cucchiara, Simone Calderara, Afshin Dehghan, and Mubarak Shah. Visual tracking: An experimental survey. *IEEE Transactions on Pattern Analysis & Machine Intelligence*, (1):1, 2013.
- [48] Daniel Streller, K Furstenberg, and Klaus Dietmayer. Vehicle and object models for robust tracking in traffic scenes using laser range images. In *Intelligent Transportation Systems, 2002. Proceedings. The IEEE 5th International Conference on*, pages 118–123. IEEE, 2002.
- [49] Jur Van Den Berg, Stephen J Guy, Ming Lin, and Dinesh Manocha. Reciprocal n-body collision avoidance. In *Robotics research*, pages 3–19. Springer, 2011.
- [50] N. Wojke, A. Bewley, and D. Paulus. Simple Online and Realtime Tracking with a Deep Association Metric. *ArXiv e-prints*, March 2017.
- [51] Nicolai Wojke and Marcel Häselich. Moving vehicle detection and tracking in unstructured environments. In *Robotics and Automation (ICRA), 2012 IEEE International Conference on*, pages 3082–3087. IEEE, 2012.
- [52] Yu Xiang, Alexandre Alahi, and Silvio Savarese. Learning to track: Online multi-object tracking by decision making. In *Proceedings of the IEEE international conference on computer vision*, pages 4705–4713, 2015.
- [53] Kota Yamaguchi, Alexander C Berg, Luis E Ortiz, and Tamara L Berg. Who are you with and where are you going? In *Computer Vision and Pattern Recognition (CVPR), 2011 IEEE Conference on*, pages 1345–1352. IEEE, 2011.
- [54] Min Yang, Yuwei Wu, and Yunde Jia. A hybrid data association framework for robust online multi-object tracking. *arXiv preprint arXiv:1703.10764*, 2017.
- [55] Liang Zhao and Chuck Thorpe. Qualitative and quantitative car tracking from a range image sequence. In *Computer Vision and Pattern Recognition, 1998. Proceedings. 1998 IEEE Computer Society Conference on*, pages 496–501. IEEE, 1998.
- [56] Thomas Zielke, Michael Brauckmann, and Werner Von Seelen. Intensity and edge-based symmetry detection with an application to car-following. *CVGIP Image Understanding*, 58:177–177, 1993.

APPENDIX: REDUCED PROBABILITY OF TRACK LOSS
WITH BACKGROUND SUBTRACTED OBJECT
REPRESENTATION

In this report, we consider Mask R-CNN for traffic agent detection, which outputs bounding boxes and their corresponding masks. We define $\mathcal{T}_t = \{\Psi_{1:t}\}$ to be the set of positively identified states for agent p_i until time t . We denote the time since the last update to a track ID as μ . We denote the ID of p_i as α and we represent the correct assignment of an ID to p_i as $\Gamma(\alpha)$. The threshold for the Cosine metric is $\lambda \stackrel{\text{i.i.d.}}{\sim} \mathbb{U}[0, 1]$. The threshold for the track age, *i.e.*, the number of frames before which track is destroyed, is ξ . We

denote the probability of an event that uses Mask R-CNN as the primary object detection algorithm with $\mathbb{P}^M(\cdot)$ and the probability of an event that uses a standard Faster R-CNN as the primary object detection algorithm (*i.e.*, outputs bounding boxes without background subtraction) with $\mathbb{P}^F(\cdot)$. Finally, $\mathcal{T}_t \leftarrow \{\phi\}$ represents the loss of \mathcal{T}_t by occlusion.

Theorem V.1. *With probability $1 - \frac{B}{A}$, binary tensors extracted from the background subtracted (BGS) representations decrease the number of road agent tracks lost, thereby reducing the number of false negatives, in comparison to regular bounding boxes.*

Proof. We use the mask from Mask-RCNN and bounding box pair to generate a BGS representation. The correct assignment of an ID depends on successful feature matching between the predicted measurement feature and the optimal detection feature. In other words,

$$l(f_{a_i}, f_{h_j^*}) > \lambda \Leftrightarrow (\alpha = \phi) \quad (11)$$

Using Proposition V.2 and the fact that $\lambda \stackrel{\text{i.i.d.}}{\sim} \mathbb{U}[0, 1]$,

$$\mathbb{P}(l(f_{a_i}, f_{h_j^*, p_i}^M) > \lambda) < \mathbb{P}(l(f_{a_i}, f_{h_j^*, p_i}^F) > \lambda)$$

Using Eq. 1, it directly follows that,

$$\mathbb{P}^M(\alpha = \phi) < \mathbb{P}^F(\alpha = \phi) \quad (12)$$

In our approach, we set

$$(\mu > \xi) \wedge (\alpha = \phi) \Leftrightarrow \mathcal{T}_t \leftarrow \{\phi\}$$

Using Eq. 2, it follows that,

$$\mathbb{P}^M(\mathcal{T}_t \leftarrow \{\phi\}) < \mathbb{P}^F(\mathcal{T}_t \leftarrow \{\phi\}) \quad (13)$$

We define the total number of false negatives (FN) as

$$FN = \sum_{t=1}^T \sum_{p_g \in \mathcal{G}} \delta_{\mathcal{T}_t} \quad (14)$$

where $p_g \in \mathcal{G}$ denotes a ground truth pedestrian in the set of all ground truth pedestrians at current time t and $\delta_z = 1$ for $z = 0$ and 0 elsewhere. This is a variation of the Kronecker delta function. Using Eq. 3 and Eq. 4, we can say that fewer lost tracks ($\mathcal{T}_t \leftarrow \{\phi\}$) indicate a smaller number of false negatives. ■

The upper bound, $\mathbb{P}^F(\mathcal{T}_t)$, in Eq. 3 depends on the amount of padding done to f_{a_i} and f_{h_j} . A general observed trend is that a higher amount of padding results in a larger upper bound in Eq. 3.

Proposition V.2. *For every pair of binary tensors ($f_{h_j}^M, f_{h_j}^F$) generated from a BGS-Representation and a bounding box respectively, if $\|f_{h_j}^M\|_0 > \|f_{h_j}^F\|_0$, then $l(f_{a_i}, f_{h_j}^M) < l(f_{a_i}, f_{h_j}^F)$ with probability $1 - \frac{c_1}{c_2}$, where A and B are positive integers and $c_1 > c_2$.*

Proof. Using the definition of the Cosine metric, the lemma reduces to proving the following,

$$f_{a_i}^T (f_{h_j}^M - f_{h_j}^F) > 0 \quad (15)$$

We pad both $f_{h_j}^M$ and $f_{h_j}^F$ such that $\|f_{h_j}^M\|_0 > \|f_{h_j}^F\|_0$.

We reduce $f_{p_i}^T, f_{h_j}^M$, and $f_{h_j}^F$ to binary vectors, *i.e.*, vectors composed of 0s and 1s. Let $\Delta f = f_{h_j}^M - f_{h_j}^F$. We denote the number of 1s and -1 s in Δf as c_1 and c_2 , respectively. Now, let x and y denote the L_0 norm of $f_{h_j}^M$ and $f_{h_j}^F$, respectively. From our padding procedure, we have $x > y$. Then, if $x = c_1$, and $y = c_2$, we trivially have $A > B$. But if $y > c_2$, then $c_1 = x - (y - c_2) \Rightarrow c_1 - c_2 = x - y$. From $x > y$, it again follows that $c_1 > c_2$. Thus, $x > y \Rightarrow c_1 > c_2$.

Next, we define a $(1, 1)$ coordinate in an ordered pair of vectors as the coordinate where both vectors contain 1s. Similarly, a $(1, -1)$ coordinate in an ordered pair of vectors is the coordinate where the first vector contains 1 and the second vector contains -1 . Then, let p_a and p_b respectively denote the number of $(1, 1)$ coordinates and $(1, -1)$ coordinates in the pair $(f_{p_i}^T, \Delta f)$. By definition, we have $0 < p_a < c_1$ and $0 < p_b < c_2$. Thus, if we assume p_a and p_b to be uniformly distributed, it directly follows that $\mathbb{P}(p_a > p_b) = 1 - \frac{c_2}{c_1}$. ■